Lennox, A. J. J., Bartels, P., Pohl, M. M., Junge, H., & Beller, M. (2016). In situ photodeposition of copper nanoparticles on TiO_2: Novel catalysts with facile light-induced redox cycling. *Journal of Catalysis*, *340*, 177-183. https://doi.org/10.1016/j.jcat.2016.04.011

In situ Photodeposition of Copper Nanoparticles on TiO_2: Novel Catalysts with Facile Light-Induced Redox Cycling

Alastair J. J. Lennox,[a] Petra Bartels,[a] Marga-Martina Pohl,[a] Henrik Junge[a] and Matthias Beller[a]*

Leibniz Institute for Catalysis at the University of Rostock, Albert Einstein-Straße 29a, 18059 Rostock, Germany.

E-mail: matthias.beller@catalysis.de (M. Beller)

Keywords: copper • titania • hydrogen • photocatalysis • nanoparticles • photodeposition

Abstract: The *in situ* photodeposition method of copper(0) nanoparticles on TiO_2 is found to produce photoactive heterogeneous catalysts suitable for redox reactions. Several variables in the method that effect catalyst structure and activity have been investigated for H_2 generation as a model reaction. The counter-anion of the copper salt used plays a pivotal role in determining size, distribution and crystallinity of the nanoparticles, as well as leaching, recyclability and stabilisation. Redox cycling between Cu(0) and Cu(II) was found to be extremely facile, with oxidation occurring aerobically and re-reduction under anaerobic irradiation in water.

1. Introduction

Photon-excitable heterogeneous materials are a rapidly growing class of catalyst for effecting chemical transformations. As well as the clear energy savings from adopting photochemical conditions over conventional heating, employing heterogeneous materials allows the possibility of catalyst recovery and reuse. For these reasons, this class of catalyst is currently growing in popularity in the field of synthetic methodology.[1–5] Additionally, photochemical conditions can often engender unique reactivity that is different under thermal or electrochemical conditions, thus widening the plethora of organic transformations available. Their use in photocatalytic water-purification is also well established,[6,7] where persistent organic compounds and microorganisms can be efficiently degraded. However, photon-active heterogeneous semi-conductors have been most extensively studied in water-splitting,[8–14] where they show great potential in reducing and oxidizing water to generate hydrogen and oxygen gas, respectively, for their use in fuel cells.

Metal nanoparticles supported on heterogeneous semiconductors have proven to be especially successful co-catalysts for each of these applications.[15,16] Success has been achieved by deposition of noble metals, such as gold[17–19] or platinum,[19–21] mounted on photoactive supports, such as CdS,[22] Fe_2O_3,[23] or WO_3,[24] but most commonly onto TiO_2,[25] due to its high chemical inertness and stability towards photochemical decay. The co-catalyst aids in attenuation of charge recombination following photon-induced charge excitation and separation.[26] Under UV-irradiation, electron-pooling in the metal occurs as a result of Schottky barrier formation at the metal–semiconductor interface, and thus the nanoparticle serves as the redox reaction centre. Visible light absorption may be enhanced by the surface

plasmon resonance (SPR) effect, which is caused by the oscillation of the conduction electrons in surface bound metal atoms under visible light illumination.[17,27–28]

To improve the economic viability of their use, it is desirable to replace the expensive noble metal with a more available non-noble metal, such as copper. Despite reports of a reduction in activity with copper doping in the TiO_2 lattice,[29] when Cu nanoparticles are deposited onto the TiO_2 surface the materials become interesting catalysts for water[29–42] and CO_2[43] reduction, as well as water-gas-shift[44a] and water purification.[44b] So far, a number of methods to deposit copper onto supports, such as deposition-precipitation,[32,37] sol-gel immobilisation,[31,45,46] wet[29,31,33,37,38,41,42] or ion[30] impregnation, chemical reduction[31] and photodeposition are known.[31,47] It is clear that the oxidation state, surface and bulk deposition coverage, nanoparticle size and distribution are all dependent on the preparation method. Thus, each method can produce novel and unique catalysts with different properties, which can each be optimal for different applications.[31,46] The structural variation attained from each preparation method determines the nature of the nanoparticles and their interaction with the support, thus demonstrating the importance of analysing the structure and assessing the properties of catalysts prepared in different ways.

Despite the method being established in the case of gold,[48] ***in situ*** photodeposition of copper, to the best of our knowledge, has not received any attention. Advantageously, in this method, the constituent parts are added to the reaction mixture, and the active catalyst is formed under the photocatalytic conditions without the necessity for isolation, calcination or purification. The lack of attention is especially surprising considering its simplicity, making it well suited for use in a range of procedures, including energy, as well as synthetic applications. As the catalyst is not isolated, the preparation conditions become more important, and, in order for the field to expand, a greater understanding of the important variables to this technique is necessary. In addition, characterisation of the relationships between structure and reactivity will greatly enhance development. Herein, we identify a number of important features of *in situ* photodeposition of copper nanoparticles on TiO_2, the catalysts it generates and the relationship between these features to their activity.

2. Materials and Methods

2.1. Materials

TiO_2 (Hombikat) and all copper salts were purchased from Sigma Aldrich and used without further purification. Distilled water was saturated with argon, methanol was passed through a column of anhydrous alumina before being distilled from magnesium under argon. Deuterated solvents for NMR analysis were purchased from Euriso-Top. The lamp used throughout was a LOT (LSB530) 300 W Xe lamp, calibrated to 1.5 W at 10 cm with no additional filter.

2.2. Catalyst preparation

Catalysts were prepared *in situ* by addition of a copper salt stock solution (6 μmol of Cu) in methanol (5 mL) under an inert atmosphere of argon gas. This stock solution was added to the double-walled, thermostatically controlled,

reaction vessel containing a stir bar and TiO_2 (25 mg) over a counter flow of argon gas. To this was added water (5 mL) and the reaction was stirred for 5 min.

2.3. Catalytic proton reduction reactions

A double-walled, thermostatically controlled (at 25.0 °C), reaction vessel was connected *via* a condenser to an automatic gas burette. The gas burette was equipped with a pressure sensor. Evolving gas during the reaction causes a pressure increase in the closed system, which is compensated by a volume increase of the burette syringe by an automatic controlling unit. The increase in volume was recorded every 0.5 min and the data collected on a computer. A GC sample was taken from the collected gas in the burette after each reaction to determine the gaseous composition. GCs were calibrated with certified commercially available gas mixtures.

2.4. Catalyst isolation

Following completion of a reaction, the catalyst was isolated by transferring the reaction mixture to a centrifuge flask, washing with extra portions of MeOH. It was centrifuged (3000 rpm) for 25 min and the solid isolated from the solvent by decantation. The catalyst was washed with a further portion of MeOH:water (1:1), centrifuged, and separated again from the solution. If the catalyst was being analysed then it would be thoroughly dried first. If the catalyst was being recycled then it would be transferred into a new reaction flask, using the new reaction solvent to aid complete transfer.

2.5. Catalyst Characterisation

ICP-OES. For determining the composition by *ICP-OES*, a Varian 715-ES ICP optical emission spectrometer was used. The aqueous samples (10 mL) were diluted 1: 100 or 1: 1000 and made up to 25 mL. The data analysis was performed using the Varian 715-ES Software "ICP Expert".

TEM. Measurements were performed at 200 kV with an aberration-corrected JEM-ARM200F (JEOL, Corrector: CEOS). The microscope is equipped with a JED-2300 (JEOL) energy-dispersive X-ray-spectrometer (EDXS) for chemical analysis. The aberration corrected STEM imaging (High-Angle Annular Dark Field (HAADF) and Annular Bright Field (ABF)) were performed under the following conditions. HAADF and ABF both were done with a spot size of approximately 0.13nm, a convergence angle of 30-36° and collection semi-angles for HAADF and ABF of 90-170 mrad and 11-22 mrad, respectively. Preparation of the TEM sample: The solid samples to be analysed were prepared without any pre-treatment by deposition of the solid on a holey carbon supported Ni-grid (mesh 300) and transferred to the microscope. In the case of suspensions, one drop was deposited on the carbon supported grid. The excess of suspension was removed after 10 seconds.

XPS. The oxidation states and the surface composition were determined by X-ray photoelectron spectroscopy (XPS). The measurements were performed with an ESCALAB 220iXL (ThermoFisher Scientific) with monochromatic Al K_α radiation (E = 1486.6 eV). The samples were fixed on a stainless steel sample holder with double adhesive carbon tape. For charge compensation a flood gun was used, the spectra were referenced to the Ti 2p 3/2 peak of TiO_2 at 458.8 eV. After background subtraction, the peaks were fitted with Gaussian-Lorentzian curves to determine the positions and the

areas of the peaks. The surface composition was calculated from the peak areas divided by the element-specific Scofield factor and the transmission function of the spectrometer.

AAS. The AAS device (AAnalyst 300 Perkin Elmer) is a computer controlled routine atomic absorption and emission spectrometer for flame AAS, with double-beam optics (Deuterium lamp and hollow-cathode lamp), 6-fold lamp changer, burner system for air/acetylene (temperature 2150-2400 °C) and nitrous oxide/acetylene (temperature 2650-2800 °C) and safe gas supply.

NMR. ^{19}F NMR spectra were recorded on a *Varian 400* spectrometer. Quantification of PF_6^- and BF_4^- anions in solution following separation from the solid catalyst was made by normalisation of the peak area a known amount of added pentafluorophenol.

UV/vis. The diffuse reflectance UV/vis spectra were recorded on an AvaSpec-2048 (avantes) equipped with an avantes AvaLight-DH-S-BAL deuterium lamp.

Further details on the Materials and Methods can be found in the Supplementary Material file

3. Results and Discussion

3.1. Initial development

The catalysts generated *in situ* from different copper precursors and under different conditions were studied in the photocatalytic water reduction. This model reaction was chosen, not only because it is a simple and highly important reaction, but the generation of gas, which can be collected and measured in an automatic burette, allows for a straightforward and rapid on-line assessment of the catalyst proficiency. In the presence of a suitable hole-scavenger the structural details presented should be relevant to other reactions and applications. In each case, a copper precursor and TiO_2 (25 mg) were added to a solution of water and methanol, as hole scavenger,[49] (10 mL, 1:1[50]). Initial studies confirmed a steady evolution of H_2 with minor quantities of CO (<0.16%) and CO_2 (<1.0%) originating from quenching of the photo-generated holes by methanol on the excited-state semi-conductor.[51,52] Control reactions confirmed that in the absence of TiO_2 or Cu no active catalyst was formed, Figure 1, and that the presence of both methanol and water are essential.[53] Thus, we propose UV/vis-light excites an electron from the valence to the conduction band of TiO_2. Electron-pooling in the co-catalytic copper nanoparticles attenuates charge recombination and provides the site of proton reduction and subsequent H_2 gas formation.[26]

3.2. Copper loading

It is important to study the effect of copper loading on reactivity. An increase in the number of active sites can increase the activity, but an optimum metal particle size is required, without blocking light to TiO_2.[41] Indeed, a peak in performance was observed using 6 μmol of $Cu(acac)_2$, Figure 1. Under these conditions the reaction rate was maintained over an extended period and up to the collection limit of our equipment.[53] Subsequent studies were performed using this optimum catalyst composition. In all cases no induction periods were observed, suggesting an

extremely rapid reduction and deposition process. The effect of lamp power was also tested and predictably led to increases in reaction rate. The effect of light intensity has previously been shown by TEM measurements to be negligible on particle sizes,[48] proving it is merely a kinetic effect.

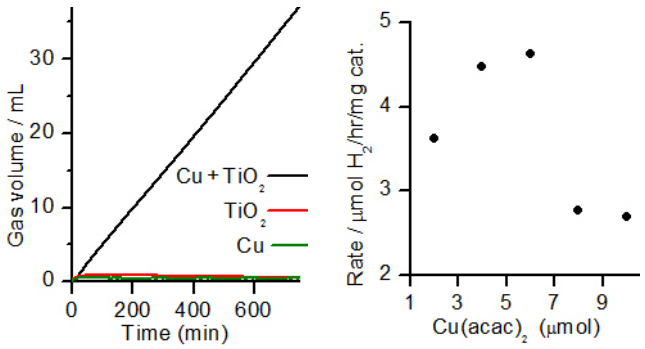

Figure 1. H_2 evolution from *in situ* generated photodeposition of Cu on TiO_2. Left: Black line: $Cu(acac)_2$ (6 µmol), TiO_2 (25 mg), water:methanol (1:1 v:v, 10 mL), 300 W Xe-lamp (output 1.5 W), 25 °C, red: same as black but without Cu; Green: same as black but without TiO_2. Right: rate vs quantity of Cu precursor.

3.3. Oxidation state determination and cycling

Under the inert (Ar) reaction conditions, catalyst mixtures consistently turned dark purple in colour, which was suspected to be due to formation of Cu(0) nanoparticles. Upon exposure to air, the solutions slowly turned white, a process that would be consistent with Cu oxidation. Returning the solution to inertion and light irradiation at 25 °C triggered the reverse colour change back to purple and the cycle was found to be easily amenable to many repetitions. The oxidation states of this cycle were confirmed in the following manner. A catalyst generated from the photodeposition of $[Cu(MeCN)_4]PF_6$ on TiO_2 was rapidly prepared for analysis by Energy-dispersive X-ray spectroscopy (EDX), which directly confirmed the presence of Cu(0) in the purple solid.[53] A catalyst prepared from the same copper salt was isolated after allowing the solution to turn white in air and analysed by X-ray fluorescence spectroscopy (XRF), which confirmed the presence of Cu(II)O. In addition to this, X-ray photoelectron spectroscopy (XPS) was also used to compare 2 catalysts, prepared in the same way, now from $Cu(NO_3)_2{\cdot}3H_2O$, but isolated differently. The first was isolated under aerobic conditions and clearly showed the presence of Cu(II), Figure 2, whose signal was absent in the second sample that was isolated under inert conditions.[54] Therefore, we can confirm that copper oxide species not do exist under the reaction conditions and that the active Cu is in oxidation state 0.

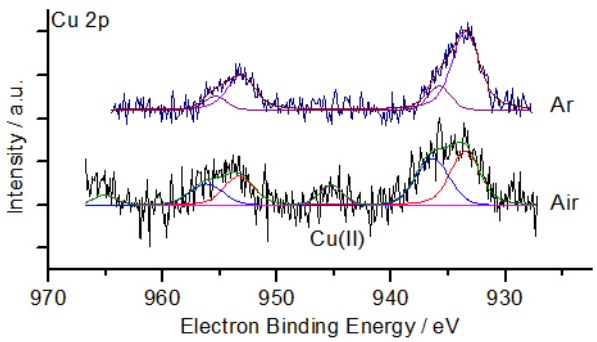

Figure 2. XP spectra showing catalysts prepared from the photodeposition of $Cu(NO_3)_2{\cdot}2H_2O$ (6 μmol) on TiO_2 (25 mg) in MeOH:water (1:1 v:v, 10 mL), 20 hr irradiation 1.5 W output Xe-lamp, isolated under, upper, inert conditions and, lower, aerobic conditions.

The effect of this redox cycling was tested on the catalyst activity. The apparatus was fitted with a tap to isolate the burette from the reaction mixture. The tap was closed periodically to allow the reaction exposure to air and with the light switched off it turned to its characteristic white colour. Following argon purging and irradiation, the reaction returned to purple and the tap was opened again to the burette. This redox cycling was repeated 5 times over a period of 48 hours and in all cases no drop in catalytic activity was observed, Figure 3, thus demonstrating no significant structural changes to the nanoparticles despite the redox change and complete re-reduction of the oxide coating. This remarkably facile light-induced redox cycling of Cu nanoparticles observed here is an important feature of these catalysts that holds great potential to be exploited in other applications.[55] If Cu(0) is required in the catalyst then it should be stored under inert conditions, otherwise *in situ* reduction, as shown, can readily generate the active form.

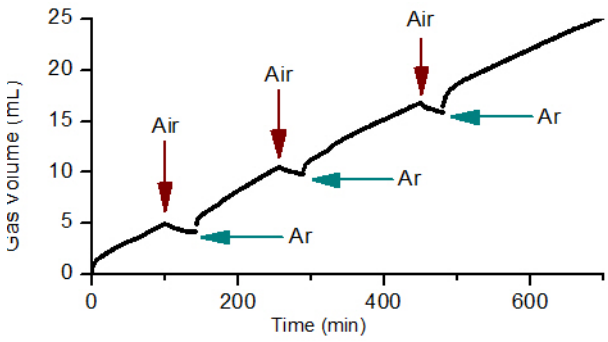

Figure 3. The first three redox cycles of Cu nanoparticles on TiO_2, indicating no clear change in the rate of gas evolution and thus the catalyst activity and its basic structure.

3.4. Copper salt dependence on reaction rate

Next, the influence of the copper salt employed for *in situ* photodeposition onto TiO_2 was investigated by screening 17 different salts (6 μmol) and monitoring the rate of reaction. The range of catalyst activity was found to be

extremely influenced by the copper precursor, Figure 4, as rates varied by a factor of 50 from 0.09 μmol/hr/mg cat to 4.24 μmol/hr/mg cat, which equates to a difference of about 30 mL of H_2 after 10 hr (with 25 mg of catalyst and 1.5 W Xe-lamp). Despite the rate being slightly lower than those observed with Au and Pt,[48] due to the fact Cu is considerably cheaper than Au and Pt, the rate of H_2 production per hour per € of catalyst is 81 and 30 times higher, respectively.[53]

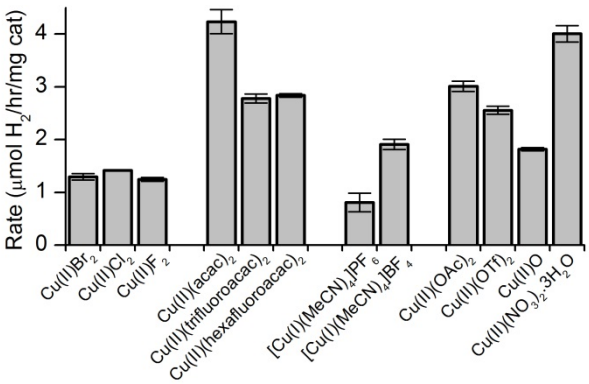

Figure 4. Rates of H_2 evolution from catalysts generated *in situ* from a selection of the different copper salts. See SI for all salts tested. Conditions: Cu salt (6 μmol), TiO_2 (25 mg), water:methanol (1:1 v:v, 10 mL), 300 W Xe-lamp (output 1.5 W), 25 °C. Rates are averages of at least 2 runs.

Copper(I) sources also gave mixed results, as the iodide salt produced an inactive catalyst whereas the chloride salt a highly active (2.71 μmolH_2/hr/mg cat)[53] one. Copper(I) oxide was only sparingly soluble in the reaction medium and therefore photodeposition onto TiO_2 did not occur immediately. After a lag time (3 hr) the characteristic Cu(0) purple solution was formed and was coupled with the initiation of a steady generation of H_2 gas. It is possible that this time taken is for its disproportionation, dissolution and TiO_2 photodeposition.

Cationic Cu(I) complexes ligated by neutral acetonitrile proved to be far more amenable to the conditions and gave reasonable rates of hydrogen gas production. Interestingly, the counter anion of the complex played an important role in determining the rate. Consistent and reproducible differences were observed when BF_4^- (1.91 μmol/hr/mg cat) was replaced by PF_6^- (0.81 μmol/hr/mg cat), equating to a difference of about 8 mL H_2 gas in 10 hr with 25 mg catalyst. A catalyst prepared using each Cu salt was isolated and analysed by transmission electron microscopy (TEM) to gain a further understanding into the origins of this remarkable effect. The larger and more diffuse PF_6^- anion,[56] which gave slower rates of reaction, produced nanoparticles of Cu(0) that were in the range of 20-40 nm. The smaller BF_4^- anion, which gave higher rates of reaction, produced smaller nanoparticles in the range of 10-20 nm, Figure 5. Despite other factors being at play, it is recognised that smaller particles sizes tend to provide higher rates of proton reduction, and can also determine the wavelength dependent electron transfer mechanism.[27a] When comparing Cu(0) particles of roughly the same size generated from the two salts, a difference was also observed in the number of corner and edge atoms present. The more active catalyst, from BF_4^-, possessed *less* corner and edge atoms and larger crystallites than the less active catalyst, from PF_6^-, Figure 6.

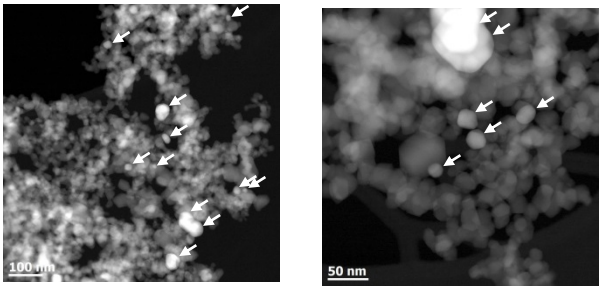

Figure 5. Left HAADF image of: less active catalyst with larger Cu(0) particles, mostly between 20-40 nm, generated under the general conditions using $[Cu(MeCN)_4PF_6]$, scale bar = 100 nm. Right: HAADF image of more active catalyst with smaller Cu(0) particles, mostly between 10-20 nm, generated under the general conditions using $[Cu(MeCN)_4BF_4]$, scale bar = 10 nm. White arrows point towards copper particles.

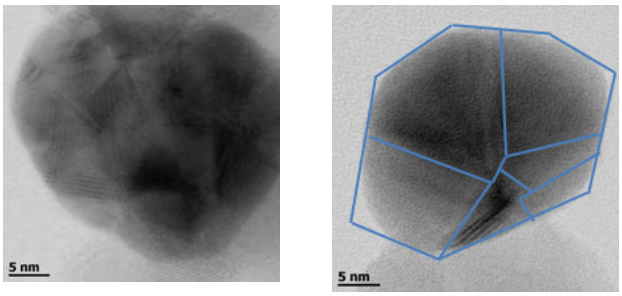

Figure 6. Left: ABF image of less active catalyst showing multifaceted polycrystalline Cu(0) particle on TiO_2 generated under the general conditions from $[Cu(MeCN)_4PF_6]$. Right: ABF image of more active catalyst showing a particle of Cu(0) with less crystallites and less facets generated under the general conditions from $[Cu(MeCN)_4BF_4]$. Added lines are a visual aid. See SI for FFT diffractograms.

This is surprising as it is commonly assumed that the active sites are the coordinatively unsaturated metal atoms (corner, edge and defects).[57,58] However, an investigation by Chen,[59] reported that identifying surface facets alone was insufficient and that surface defects play more dominant roles in determining reactivity. The defect's abundance and distribution "is strongly affected by the nanocatalyst growth pattern and synthesis procedure". Thus, these observations may be evidence that the anion can influence Cu nanoparticle growth rate, which in turn causes a difference in the state of surface defects and therefore of the catalyst activity.[60]

The use of Cu(II) salts, in general, provided catalysts with slightly increased, and more reproducible, activities than Cu(I) salts. The difference in reduction potential to Cu(0) may play a part by affecting the rate of particle growth and therefore the particle size and abundance of surface defects. However, of course, within the Cu(II) series, the nature of the counter-anion itself also has a profound influence on the rate, Figure 4. Retaining structural similarity, but decreasing electron density at copper was conveniently tested by comparing catalysts generated using acetylacetonate (acac), trifluoro-acac and hexafluoro-acac ligands. A significant drop in activity was observed with the use of trifluoro-acac compared to acac. Increasing the effect further to hexafluoro-acac did not lead to any further significant changes. This trend was also observed when comparing Cu(II) acetate with Cu(II) triflate, as the more stable conjugate base

provides access to a less active catalyst. However, there was no meaningful difference when comparing Cu(II) halide salts. Much higher and reproducible rates were achieved employing $Cu(NO_3)_2 \cdot 3H_2O$ as copper source. Finally, very stable Cu complexes ligated by phthalocyanine or NHC ligands did not achieve high activity.[53]

As demonstrated, *vide supra*, it is surprising how simple differences in the anion (*e.g.* PF_6^- vs BF_4^-) can significantly influence catalyst structure and activity (hydrogen evolution rates). A reasonable rationale for these differences is in the strength of its interaction to Cu, which will affect its ability to seed and crystallise, the rate of nanoparticle formation and defect growth. Also, organic counter anions can potentially be oxidized by holes that would contribute to, and possibly enhance, H_2 production. Indeed, there is also the possibility of the anion being included in the catalyst structure. Indeed, XP spectroscopy of a catalyst prepared using $Cu(NO_3)_2 \cdot 3H_2O$ confirmed the presence of nitrogen in the isolated, washed and dried solid.[53] The high rates observed using this catalyst sustained after being recycled, *vide infra*, may be explained by nanoparticle stabilisation through anion incorporation. However, this is, of course, not the case for all anions. PF_6^- and BF_4^- were detected (^{19}F NMR) in the solution phase of separated catalyst mixtures prepared using $[Cu(MeCN)_4PF_6]$ and $[Cu(MeCN)_4BF_4]$, respectively.

3.5. Copper deposition and leaching

The counter-anion was found to have a strong influence on the quantity of copper that is photodeposited on TiO_2 and also the amount of leaching into solution. Photocorrosion and re-deposition will have an influence on the catalyst activity by regenerating the Cu surface and particle dispersion. The activity of catalysts generated from 13 different salts was tested, after which they were isolated by centrifugation, dried and analysed by Atomic Absorbance spectroscopy (AAS) for Cu loading. The separated solution was analysed by ICP-OES for its Cu content.[53] Due to the specific role of some anions in particle formation and integration into the catalyst structure, it is non-trivial to make a deep analysis of all the data. Nevertheless, several trends are clear. Increasing fluorination in acac decreases Cu leaching from 10% down to 0%, whilst at the same time, increasing the Cu deposited on TiO_2 from 0.56 – 1.22%. There was no Cu leaching detected, and almost the highest quantity of Cu deposited onto TiO_2 with the use of $Cu(NO_3)_2 \cdot 3H_2O$, which provides the most active catalyst. However, the most Cu deposited was from employing CuI or CuF_2, two fairly inactive complexes with unreproducible rates, which suggests a peak performance from a medium metal loading, which is in accordance with noble metal catalysts.[27a]

3.6. Catalyst recycling

The effect of catalyst recycling on the reaction rate was tested. Catalysts were prepared using the *in situ* photodeposition method and tested over 23 hours, isolated by centrifugation, re-tested and the cycle repeated up to 4 times. The separated solvent from each run was then analysed by ICP-OES for leached copper, Figure 7. It was observed that an increase in the activity occurred after recycling the catalysts generated from $[Cu(I)MeCN_4]^+$ with either PF_6^- or BF_4^- anions. However, further recycling did not produce any further enhancements in the rate. This is consistent with complete separation of the counter-anion (^{19}F NMR *vide supra*) after the first separation. In the case of the less active $[Cu(MeCN)_4PF_6]$, 33% of the copper was detected (ICP-OES) in solution after the first solid/solution separation.

Consistently, no more leached copper was detected upon further recycling. Interestingly, no copper leached in the case of the more active BF_4^-. Reproducible increases in activity were observed when employing $CuCl_2$ and $CuBr_2$, however, copper was again only detected in solution after the first use of these Cu salts. The trend of increasing activity was not continued when recycling the more active catalysts made from either $Cu(acac)_2$ or $Cu(NO_3)_2{\cdot}3H_2O$. In addition to this finding of anion dependent leaching, it has previously been found that more oxidizing or acidic environments also lead to a greater extent of copper leaching.[34]

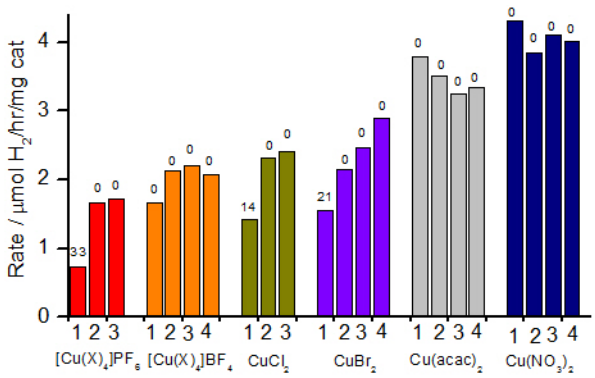

Figure 7. Rates of H_2 production from catalysts made by photodeposition of different copper salts and the effect of recycling on reaction rate. X = MeCN. Numbers below column indicate the run number and numbers above column are % Cu content detected (ICP-OES) in the solution phase after separation of the used catalyst from each run.

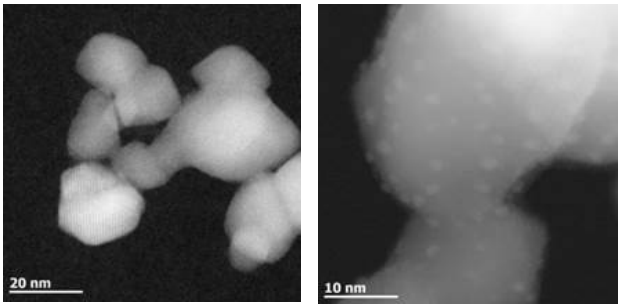

Figure 8. Left: HAADF image of catalyst made from *in situ* photodeposition of $Cu(acac)_2$ on TiO_2 and recycled 4 times; scale bar = 10 nm. Only particles of TiO_2 can be seen and no Cu is detected by this technique. Right: HAADF image of catalyst made from *in situ* photodeposition of $Cu(NO_3)_2{\cdot}3H_2O$ on TiO_2 and recycled 4 times; scale bar = 5 nm. Cu nanoparticles of less than 2 nm can clearly be seen decorating the TiO_2 particles.

In order to gain further insight into the origin of this behaviour, the solid catalysts were analysed by TEM after the final run. Surprisingly, in all cases except $Cu(NO_3)_2{\cdot}3H_2O$, no recognisable copper nanoparticles could be detected. Occasionally, sub-nanometer particles that possibly resembled copper were found but their identity could not be verified. Thus, these highly active catalysts do not have any observable Cu nanoparticles. However, the presence of copper was confirmed in two ways. Firstly, under the EDX beam Cu particles accumulated and could then be detected. Secondly, a

sample of catalyst having been recycled four times was analysed by XRF spectroscopy and found 1.08% CuO was present. Therefore, it can be concluded that recycling has the effect of reducing the particle sizes to the level where the metal is atomically distributed on the semi-conductor support. A process involving dissolution and re-reduction is invoked, which proceeds in parallel with an increase in the activity for most examples. The increase in activity is likely due to a change in mechanism, as the active incident wavelength changes with different nanoparticle sizes.[27a] In addition, high dispersity of Cu(II) leads to more rapid and extensive reduction under the reaction conditions,[36] thus producing a higher frequency of active sites. In the case of the highly active $Cu(NO_3)_2{\cdot}3H_2O$ salt, evenly distributed particles below 2 nm were still observed after the final recycle, indicating this catalyst to be stable as its dissolution is particularly disfavoured.

4. Conclusions

In summary, we have examined the effects on catalyst structure and reactivity of several variables in the *in situ* photodeposition method of copper on TiO_2 surface. The reduction of water to hydrogen was employed as a model reaction. Cu(0) was identified as the active reduction site under the reaction conditions, but redox cycling between Cu(0) and Cu(II) was found to be facile, with oxidation occurring aerobically and re-reduction under irradiation. We anticipate this effect could be highly useful, as this novel reactivity can be integrated into redox catalysis in organic methodologies. The copper salt and counter-anion used were found to be extremely important, both to catalyst structure and its activity. *The most active catalyst came from the use of $Cu(II)(NO_3)_2{\cdot}3H_2O$ (6 µmol), TiO_2 (25 mg) in MeOH:water (1:1 v:v) - copper did not leach, formed small particles (<2 nm) and gave reproducible rates after recycling.* Despite the complexity within the system for other copper salts,[61] a number of key observations have still been realised:

- the *in situ* photodeposition method can only occur with a soluble copper salt, under anaerobic conditions and light irradiation
- the counter-anion determines the nanoparticle size and crystallinity, the net amount of copper deposited and the degree of copper leaching into solution.
- recycling improved the activity for the less active catalysts by decreasing the nanoparticle size, but there was no significant effect on the more active catalysts, which have smaller particles loaded and may be stabilised by the anion.

In addition to establishing the *in situ* photodeposition method for copper on titania, these findings will be important in the further development and application of this class of catalyst. Uncovering the complexities and revealing structure/activity relationships is integral for heterogeneous catalysis to be applied in new fields.

Acknowledgements

We would like to thank Dr. J. Radnik for XPS, Dr. C. Kreyenschulte for TEM, A. Lehmann for AAS, A. Simmula for ICP-OES and Dr. A.-E. Surkus for DPV measurements and Dr. N. Rockstroh for proof reading the manuscript. A.J.J.L would

like to thank the Alexander von Humboldt Foundation for generous funding. This work has also been funded by the Deutsche Forschungsgemeinschaft (DFG-SPP 1613).

Appendix A. Supplementary material Supplementary data associated with this article can be found, in the online version, at …

[1] G. Palmisano, V. Augugliaro, M. Pagliaro L. Palmisano, Chem. Commun. (2007) 3425–3437.
[2] X. Lang, X. Chen and J. Zhao, Chem. Soc. Rev. 43 (2014) 473–486.
[3] M. Cherevatskaya and B. König, Russ. Chem. Rev. 83 (2014) 183–195.
[4] D. Ravelli, D. Dondi, M. Fagnoni A. Albini, Chem. Soc. Rev. 38 (2009) 1999–2011.
[5] Y. Sugano, Y. Shiraishi, D. Tsukamoto, S. Ichikawa, S. Tanaka T. Hirai, Angew. Chem. Int. Ed. 52 (2013) 5295–5299.
[6] M. N. Chong, B. Jin, C. W. K. Chow and C. Saint, Water Res. 44 (2010) 2997–3027.
[7] A. Ibhadon P. Fitzpatrick, Catalysts 3 (2013) 189–218.
[8] X. Chen, S. Shen, L. Guo S. S. Mao, Chem. Rev. 110 (2010) 6503–6570.
[9] K. S. Joya, Y. F. Joya, K. Ocakoglu R. van de Krol, Angew. Chem. Int. Ed. 52 (2013) 10426–10437.
[10] T. Hisatomi, J. Kubota K. Domen, Chem. Soc. Rev. 43 (2014) 7520–7535.
[11] K. Maeda, J. Photochem. Photobiol. C, 12 (2011) 237–268.
[12] K. Iwashina, A. Iwase, A. Kudo, Chem. Sci. 6 (2015) 687
[13] a) M. Ashokkumar, Int. J. Hydrogen Energ. 23 (1998) 427–438; b) Y. Horiuchi, T. Toyao, M. Takeuchi, M. Matsuoka M. Anpo, Phys. Chem. Chem. Phys. 15 (2013) 13243–13253.
[14] Y. Ma, X. Wang, Y. Jia, X. Chen, H. Han C. Li, Chem. Rev. 114 (2014) 9987–10043.
[15] S. K. Dutta, S. K. Mehetor N. Pradhan, J. Phys. Chem. Lett. 6 (2015) 936–944.
[16] J. Yang, D. Wang, H. Han C. Li, Acc. Chem. Res. 46 (2013) 1900–1909.
[17] J. B. Priebe, M. Karnahl, H. Junge, M. Beller, D. Hollmann A. Brückner, Angew. Chem. Int. Ed. 52 (2013) 11420–11424.
[18] J. B. Priebe, J. Radnik, A. J. J. Lennox, M.-M. Pohl, M. Karnahl, D. Hollmann, K. Grabow, U. Bentrup, H. Junge, M. Beller A. Brückner, ACS Catal. 5 (2015) 2137–2148.
[19] G. R. Bamwenda, S. Tsubota, T. Nakamura M. Haruta, J. Photochem. Photobiol. A 89 (1995) 177–189.
[20] H. Liu, J. Yuan W. Shangguan, Energy Fuels 20 (2006) 2289–2292.
[21] A. Galińska J. Walendziewski, Energy Fuels. 19 (2005) 1143–1147.
[22] K. Zhang L. Guo, Catal. Sci. Technol. 3 (2013) 1672.
[23] J. Wang, S. Pan, M. Chen D. A. Dixon, J. Phys. Chem. C 117 (2013) 22060–22068.
[24] C. Janáky, K. Rajeshwar, N. R. de Tacconi, W. Chanmanee M. N. Huda, Catal. Today 199 (2013) 53–64.
[25] A. L. Linsebigler, G. Lu J. T. Yates, Chem. Rev. 95 (1995) 735–758.
[26] J. Sá, M. Fernández-García, J. A. Anderson, Catal. Commun. 9 (2008), 1991–1995.
[27] a) C. G. Silva, R. Juárez, T. Marino, R. Molinari H. García, J. Am. Chem. Soc. 133 (2011) 595–602; b) J.-J. Chen, J. C. S. Wu, P. C. Wu D. P. Tsai, J. Phys. Chem. C 115 (2011) 210–216.
[28] K. Qian, B. C. Sweeny, A. C. Johnston-Peck, W. Niu, J. O. Graham, J. S. DuChene, J. Qiu, Y.-C. Wang, M. H. Engelhard, D. Su, E. A. Stach W. D. Wei, J. Am. Chem. Soc. 136 (2014) 9842–9845.
[29] N. Wu, Int. J. Hydrogen Energ. 29 (2004) 1601–1605.
[30] Y. Wu, G. Lu S. Li, Catal. Lett. 133 (2009) 97–105.
[31] S. Xu, J. Ng, X. Zhang, H. Bai D. D. Sun, Int. J. Hydrogen Energ. 35 (2010) 5254–5261.
[32] J. Yu J. Ran, Energy Environ. Sci. 4 (2011) 1364.
[33] H. Choi M. Kang, Int. J. Hydrog. Energ. 32 (2007) 3841–3848.

[34] V. Gombac, L. Sordelli, T. Montini, J. J. Delgado, A. Adamski, G. Adami, M. Cargnello, S. Bernal P. Fornasiero, J. Phys. Chem. A 114 (2010) 3916–3925.

[35] T. Montini, V. Gombac, L. Sordelli, J. J. Delgado, X. Chen, G. Adami P. Fornasiero, ChemCatChem 3 (2011) 574–577.

[36] J. M. Valero, S. Obregón G. Colón, ACS Catal. 4 (2014) 3320–3329.

[37] L. S. Yoong, F. K. Chong B. K. Dutta, Energy 34 (2009) 1652–1661.

[38] Z. Yu, J. Meng, Y. Li Y. Li, Int. J. Hydrogen Energ. 38 (2013) 16649–16655.

[39] W.-Y. Cheng, T.-H. Yu, K.-J. Chao S.-Y. Lu, ChemCatChem 6 (2014) 293–300.

[40] D. Praveen Kumar, M. V Shankar, M. M. Kumari, G. Sadanandam, B. Srinivas V. Durgakumari, Chem. Commun. 49 (2013) 9443–9445.

[41] S. Xu D. D. Sun, Int. J. Hydrog. Energ. 34 (2009) 6096–6104.

[42] W. J. Foo, C. Zhang G. W. Ho, Nanoscale 5 (2013) 759–64.

[43] a) A. Dhakshinamoorthy, S. Navalon, A. Corma, H. Garcia Energy Environ. Sci. 5 (2012) 9217-9233 and references cited therein; b) H. Nasution, E. Purnama, S. Kosela J. Gunlazuardi, Catal. Commun. 6 (2005) 313–319; c) Ş. Neaţu, J. A. Maciá-Agulló, P. Concepción, H. Garcia J. Am. Chem. Soc. 136 (2014) 15969–15976; d) K. K. Bando, K. Sayama, H. Kusama, K. Okabe H. Arakawa, Appl. Catal. A 165 (1997) 391-409; e) H. Yamashita, H. Nishiguchi, N. Kamada, M. Anpo, Y. Teraoka, H. Hatano, S. Ehara, K. Kikui, L. Palmisano, A. Sclafani, M. Schiavello, M. A. Fox, Res. Chem. Intermed. 20 (1994) 815-823.

[44] a) J. A. Rodríguez, J. Evans, J. Graciani, J.-B. Park, P. Liu, J. Hrbek J. F. Sanz, J. Phys. Chem. C 113 (2009) 7364-7370; b) N. S. Foster, A. N. Lancaster, R. D. Noble C. A. Koval, Ind. Eng. Chem. Res. 34 (1995) 3865–3871.

[45] a) T. Houzouji, N. Saito, A. Kudo, T. Sakata, Chem. Phys. Lett. 254 (1996) 109-113; b) R. López, R. Gómez M. E. Llanos, Catal. Today 148 (2009) 103–108.

[46] G. Colón, M. Maicu, M. C. Hidalgo J. A. Navío, Appl. Catal. B-Environ. 67 (2006) 41–51.

[47] a) J. W. M. Jacobs, J. Electrochem. Soc. 136 (1989) 2914–2923; b) C. Ampelli, R. Passalacqua, C. Genovese, S. Perathoner, G. Centi, T. Montini, V. Gombac, J. J. D. Jaen, P. Fornasiero, RSC Adv. 3 (2013) 21776-21788

[48] F. Gärtner, S. Losse, A. Boddien, M.-M. Pohl, S. Denurra, H. Junge M. Beller, ChemSusChem 5 (2012) 530–533.

[49] T. A. Kandiel, I. Ivanova D. W. Bahnemann, Energy Environ. Sci. 7 (2014) 1420–1425.

[50] a) A ratio previously observed to work sufficiently well to compare catalyst activities. MeOH acts as hole scavenger and not as proton source. See reference 18.

[51] J. Schneider D. W. Bahnemann, J. Phys. Chem. Lett. 4 (2013) 3479–3483.

[52] C. Xu, W. Yang, Q. Guo, D. Dai, M. Chen X. Yang, J. Am. Chem. Soc. 135 (2013) 10206–10209.

[53] See SI for more details.

[54] XPS does not differentiate clearly between Cu(I) and Cu(0), however, due to the EDX results and the greater ease with which Cu(I) compared to Cu(II) is reduced to Cu(0) (E^0 = +0.52 vs +0.34 V) (which in turn is more facile than Cu(II) reduction to Cu(I) (E0 = +0.15 V)), it is safe to assume formation of Cu(0).

[55] A. Marimuthu, J. Zhang S. Linic, Science 339 (2013) 1590–1593.

[56] The octahedral PF_6^- anion has longer bond lengths (1.81 Å - MM2 calculation) compared to the tetrahedral BF_4^- (1.54 Å - MM2) anion and so the more diffuse anion should have a looser interaction with the positively charged metal centre.

[57] G. A. Somorjai and Y. Li, Introduction to Surface Chemistry and Catalysis, Wiley, 2nd edn., 2010.

[58] G. Ertl, Reactions at Solid Surfaces, Wiley, 2009.

[59] X. Zhou, N. M. Andoy, G. Liu, E. Choudhary, K.-S. Han, H. Shen P. Chen, Nat. Nanotechnol. 7 (2012) 237–241.

[60] We also acknowledge the possiblity that the anions may act to differencially quench the holes generated upon light excitation. However, with the linear evolution rates observed and low catalyst loadings, the effect is predicted to be negligible.

[61] In addition, Differential Pulse Voltammetry (DVP) did not provide any evidence for a connection between reduction potential of the copper salt employed and activity of the catalyst.